Journal of Natural Gas Science and Engineering 95 (2021) 104113

Contents lists available at ScienceDirect

Journal of Natural Gas Science and Engineering

journal homepage: www.elsevier.com/locate/jngse

CO_2 dissolution and convection in oil at realistic reservoir conditions: A visualization study

Widuramina Amarasinghe [a,b,*], Ingebret Fjelde [a], Ying Guo [a,b]

[a] NORCE Norwegian Research Centre AS, Stavanger, 4021, Norway
[b] University of Stavanger, Stavanger, 4036, Norway

ARTICLE INFO

Keywords:
Supercritical CO_2
Convective mixing with Oil
Realistic reservoir conditions
Visualization
Enhanced oil recovery
CO_2 storage

ABSTRACT

CO_2 convective mixing has been extensively studied for CO_2 dissolution in saline water but very limited with the presence of oil. The objective of this work was to visually study the supercritical CO_2 (sCO_2) dissolution and convective mixing into oil at realistic reservoir temperature and pressure conditions with and without the presence of porous media.

A specially designed high-pressure 2D-cell was used to investigate the sCO_2 mixing into oil phases. Schlieren imaging method was used as the visualization method. The experiments were carried out at 100 bar and 50 °C using n-octane, n-decane, and crude oil as the main oils. Porous media with different permeability was prepared using glass beads.

Convective fingering was found to accelerate the mixing of CO_2 with n-octane and n-decane. It was not possible to visualize the CO_2 convective fingering in crude oil due to the low opacity of the oil phase. The CO_2 dissolution into oil phases was quite instantaneous and fast without the presence of porous media. The swelling of oil was measured as 55%, 50% and 11% for n-decane, n-octane and crude oil respectively without the presence of porous media. Boundary effects were affecting the CO_2 mixing due to the circular shape of the 2D-cell. Having a water layer below the oil layer tends to dampen the CO_2 transport from the oil phase to the water phase. CO_2 dissolution into oil saturated porous media was slower compared to that without the presence of porous media. The mixing of CO_2 was faster at higher permeability than at lower permeability. Visualization of CO_2 convective mixing/fingers inside oil-saturated porous media using a Hele-Shaw cell yet to be achieved experimentally.

1. Introduction

For the past few decades, global temperature has been rising beyond human control mainly due to Greenhouse gas (GHG) emissions. Effects of global warming have started affecting day to day life of all living beings and ecosystems on the planet (Gale and Kaya, 2003). Global organizations and different authorities have been trying to come up with directives and legalization to mitigate climate change by reducing greenhouse gas emissions (Mintzer, 1987, United Nations, 2015; European Commission, 2019). Geological storage of CO_2 of captured CO_2 through an environmentally safe path is one way to contribute to the fight against climate change (Gibbins and Chalmers, 2008).

It is very important to optimize and improve the understanding of the Carbon Capture and Storage (CCS) value chain to maximize CO_2 geological storage with minimum cost (Budinis et al., 2018). Injection of CO_2 to ongoing and abandoned oil fields is a well-identified solution for the commercial utilization of CO_2. During CO_2 injection into existing oil fields for Enhanced Oil Recovery (EOR), the added CO_2 will increase the oil recovery percentage. EOR for CO_2 utilization can also reduce a significant cost of the whole CCS value chain (Brock and Bryan, 1989; Blunt et al., 1993).

After CO_2 injection into the reservoir, CO_2 will be trapped by four mechanisms which can be identified as structural trapping, residual trapping, mineral trapping, and solubility trapping (Zhang and Song, 2014; Zhang et al., 2016; Sun et al., 2020). Solubility trapping is one of the significant mechanisms for long term CO_2 storage and EOR (Bachu, 2008; Zhang and Song, 2014). During CO_2 EOR, CO_2 dissolution in oil and/or water will result in, oil swelling, viscosity reduction, and in addition to wettability alteration by reduced pH (Sohrabi et al., 2009; Fjelde and Asen, 2010). Once the injected CO_2 is mixed with oil due to diffusion, the swelling will build up differential pressure at the pore level to move the oil drops or ganglia out of the pore space, accompanied by

* Corresponding author. NORCE Norwegian Research Centre AS, Stavanger, 4021, Norway.
E-mail address: widuramina@gmail.com (W. Amarasinghe).

https://doi.org/10.1016/j.jngse.2021.104113
Received 16 November 2020; Received in revised form 14 May 2021; Accepted 20 June 2021
Available online 28 July 2021

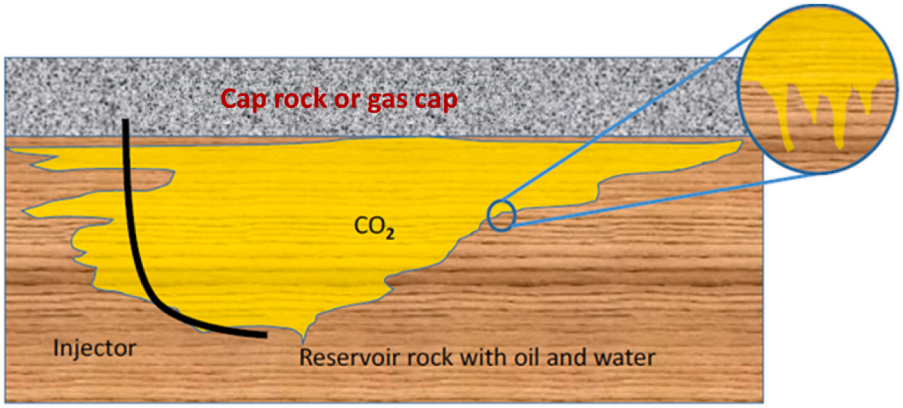

Fig. 1. Simplified sketch of convection-driving dissolution of CO_2 with oil inside the reservoir. CO_2 plume under the caprock is shown in yellow colour. Enlarge image shows how CO_2 from the plume mix with reservoir fluids.

reduced viscosity. The mixing process can be further accelerated by the gravity difference between the original oil in place and the oil-containing CO_2 which may have higher density, thus leading to the convection-driving dissolution of CO_2 as shown in Fig. 1 (Mojtaba et al., 2014; Gasda and Elenius, 2018).

The convection-driven dissolution has been extensively studied experimentally for accelerated CO_2 dissolution in saline water under gravity for CO_2 storage inside 2D Hele-Shaw cells or 3D cylindrical cells (Song et al., 2003; Neufeld et al., 2010; Kneafsey and Pruess, 2011; Khosrokhavar et al., 2014; Mojtaba et al., 2014; Vosper et al., 2014; Faisal et al., 2015; Taheri et al., 2018; Thomas et al., 2018; Mahmoodpour et al., 2019; Amarasinghe et al., 2020). Detail review of those studies can be found in Amarasinghe et al. (2020). Furthermore, numerically CO_2 convective dissolution have been studied widely with different scales and conditions (Farajzadeh et al., 2007; Hassanzadeh et al., 2009; Pau et al., 2010; Cheng et al., 2012; Elenius et al., 2014; Vosper et al., 2014; Emami-Meybodi et al., 2015; Gasda and Elenius, 2018). Elenius and Gasda (2021) have specifically investigated CO_2 convective mixing which is driven by non-monotonic density. In their numerical investigation they have investigated CO_2 convection behaviour in oil depend on its originated location. i.e. from above or below the oil zone. They have concluded that, CO_2 from above, provides a classical convective mixing with acceleration (due to viscosity decrease) while CO_2 from below flows upward (due to buoyancy), but is countered by downward convection due to the heavier mixture density. Furthermore, they have concluded that bottom convective system is notably more complex and efficient than from above.

To make the CO_2 convective flow inside fluids (water or oil) analogous to 2D, Hele-Shaw cells are used. (Hartline and Lister, 1977). Hele-Shaw cells are constructed by two parallel flat plates with a small gap in between (generally less than 10 mm). The thickness of the cell should be enough to allow a clear visualization. The Rayleigh number (Ra) should not be less than or equal $4\pi^2$ to get substantial natural convection (Lindeberg and Wessel-Berg, 1997; Faisal et al., 2015). Ra number is a dimensionless ratio between free convection to diffusion as shown in Eq. (1). Here $\Delta\rho$ is the density increase of oil and/or water due to CO_2 dissolution, g is the acceleration of gravity, k is the permeability of the porous media, H is the height of porous media or the bulk fluid, μ is the dynamic viscosity of oil or water, D is the molecular diffusion coefficient of CO_2 in oil or water and ϕ is the porosity of porous media. If a bulk fluid is being used, permeability (k) is calculated by Eq. (2) where b is the cell thickness while porosity (ϕ) is considered as 1.

$$Ra = \frac{\Delta\rho \times g \times k \times H}{\mu \times D \times \phi} \tag{1}$$

$$k = \frac{b^2}{12} \tag{2}$$

Many experimental studies have been carried out using surrogate fluids at atmospheric conditions to mimic actual CO_2 and water inside the experimental setup (Neufeld et al., 2010; Taheri et al., 2012; Tsai et al., 2013; Agartan et al., 2015; Wang et al., 2016; Teng et al., 2017). Few studies have conducted CO_2 convective dissolution in bulk water using actual CO_2 (Song et al., 2003; Kneafsey and Pruess, 2011; Khosrokhavar et al., 2014; Mojtaba et al., 2014; Faisal et al., 2015; Thomas et al., 2015; Lv et al., 2016; Lu et al., 2017; Taheri et al., 2018; Teng et al., 2018). Vosper et al. (2014) and Mahmoodpour et al. (2019) have conducted CO_2 convective dissolution into water-saturated porous media using a 2D Hele-Shaw cell under gas conditions. Amarasinghe et al. (2020) have conducted their experiments inside a Hele-Shaw cell at supercritical conditions (100 bar, 50 °C) where CO_2 was dissolved into water-saturated porous media. Wei et al. (2017) have carried out a visualization study on oil swelling due to CO_2 miscibility inside a high-pressure cylindrical cell under reservoir conditions.

However similar studies with the presence of oil (or residual oil) are still very limited. This represents a gap in defining and validating the adequate mathematical models and upscaling procedures for CO_2 storage and EOR, and the lack of input parameters for uncertainty estimation. The only study in the literature where CO_2 was convectively dissolved into the oil phase with visualization inside a Hele-Shaw cell, was conducted by Khosrokhavar et al. (2014). In their study, they have used a high-pressure cell which is made from two glass windows of 2.5 cm diameter and a thickness of 11.6 mm. They have visualized gravity-induced convective dissolution fingers of CO_2 into the n-decane phase by the Schlieren visualization method at 39 °C and 64 bars where CO_2 behaves as a sub-critical phase. They have observed a highly unstable and turbulent behaviour when CO_2 comes in contact with the oil phase. But clear distinguishable fingers are hard to identify in their images probably due to the small diameter of the cell and/or usage of a black and white camera. So they have left further interpretation of the results and images as further work. Amarasinghe et al. (2021b) have investigated CO_2 breakthrough time through an oil-saturated unconsolidated porous media at 50 °C/100 bar due to CO_2 convective mixing. They have used n-decane and crude oil with different permeable porous packs and have come up with a relationship between Ra number and dimensionless time and Ra number and CO_2 transport rate. Furthermore, they have experimentally found out that pressure decay in the CO_2-crude oil system is very low compared to the CO_2-n-decane system. Doranehgard and Dehghanpour (2020) and (Yassin et al., 2018) have visually investigated nonequilibrium CO_2/oil interactions at CO_2/oil surfaces at reservoir conditions. They have investigated oil swelling as well as CO_2 convective fingers around the CO_2/oil interface.

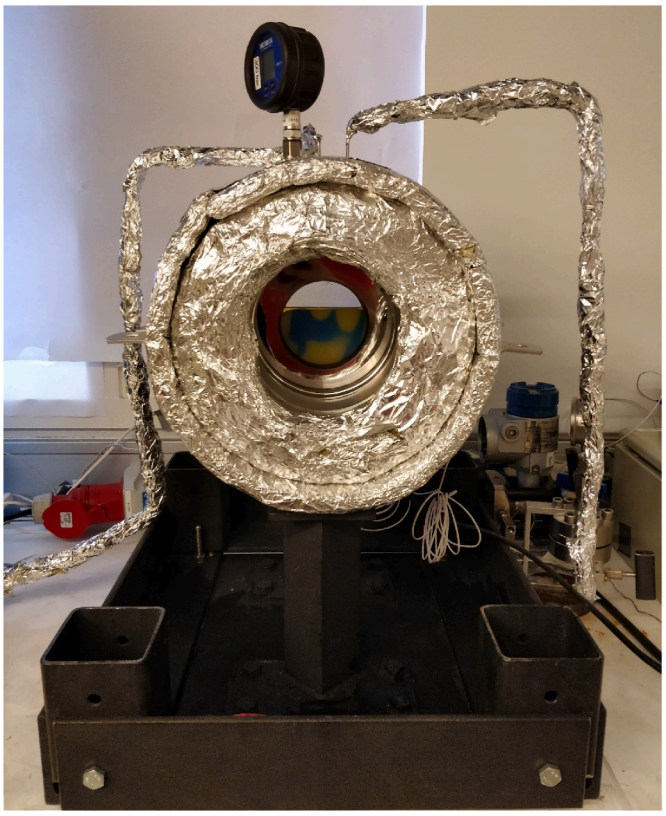

Fig. 2. Front view of the actual experiment setup.

Furthermore, they have observed that immediate oil expansion upon introduction with CO_2 and they have observed that sCO_2 provide larger oil expansion compared to liquid and gaseous CO_2. Zhao et al. (2011) have investigated and visualized CO_2 flooding in porous media inside a high-pressure PVT cell at 85 bars and 40 °C using MRI technology. Meanwhile, Seyyedsar and Sohrabi (2017) have visually investigated the formation of a new oil phase during immiscible CO_2 injection into heavy oil-saturated porous media under reservoir conditions. Liu et al. (2016) have experimentally investigated CO_2 diffusion into bulk n-decane and n-decane saturated porous media using micro-CT visualization. They have found out that initial pressure has a significant effect on the diffusion coefficient. Furthermore, due to the complications of the diffusion path in n-decane saturated porous media, they have found out that CO_2 mass transfer and diffusion coefficient reduces. Czarnota et al. (2018) and (Janiga et al., 2020) have investigated CO_2 mass transfer into the oil phase at reservoir conditions. They have used acoustic pulse-echo techniques to measure the oil volume expansion due to the CO_2 solubility in the oil phase. Meanwhile, Rezk and Foroozesh (2018) have estimated mass transfer parameters numerically for CO_2-crude oil systems. They have considered the oil swelling effect with a moving boundary and estimated that mass transfer co-efficient, diffusion co-efficient and oil swelling percentage are higher in light oil-CO_2 systems compared to heavy oil-CO_2 systems. Mahzari et al. (2018, 2019) have experimentally investigated CO_2 EOR efficiency though carbonated water injection using a micromodel system with the presence of live oil. They have visually confirmed CO_2 transfer into resident oil and eventual swelling of oil phases. Meanwhile, Amarasinghe et al. (2021a) have conducted CO_2 convective mixing visualization experiments in a micromodel apparatus using 3-phase fluid system (CO_2-water-oil) at reservoir conditions. In there, they have shown how CO_2 mixing with both diffusion and convection driven mechanism with the presence of 3-phase and how CO_2 migrate vis specific pore structures.

In this paper, we have carried out a visual investigation of CO_2 convective dissolution into oils with and without the presence of porous media inside a high-pressure 2D Hele-Shaw cell. This is the first time these kinds of experiments have been carried out in supercritical conditions using oil. Furthermore, in this study we have investigated CO_2 convective fingering in detail compared to Khosrokhavar et al. (2014).

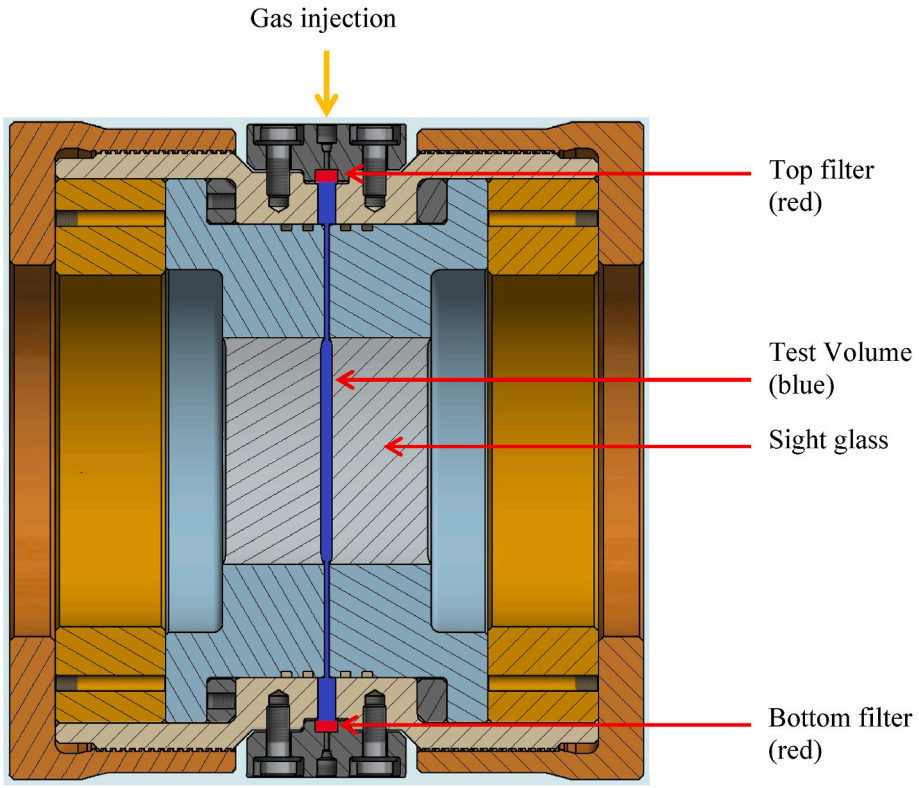

Fig. 3. Cross-section of the high-pressure cell highlighting the test volume, filter locations and gas injection location.

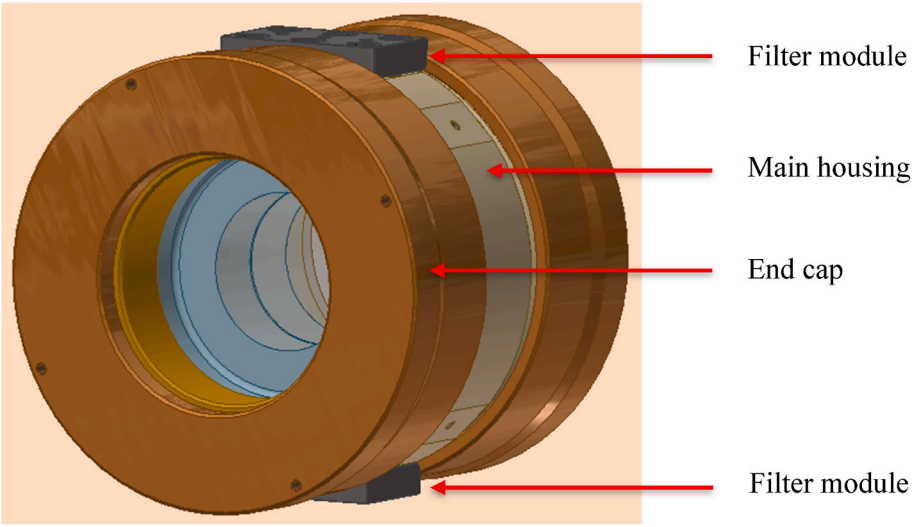

Fig. 4. 3D sketch of the high-pressure cell including main components.

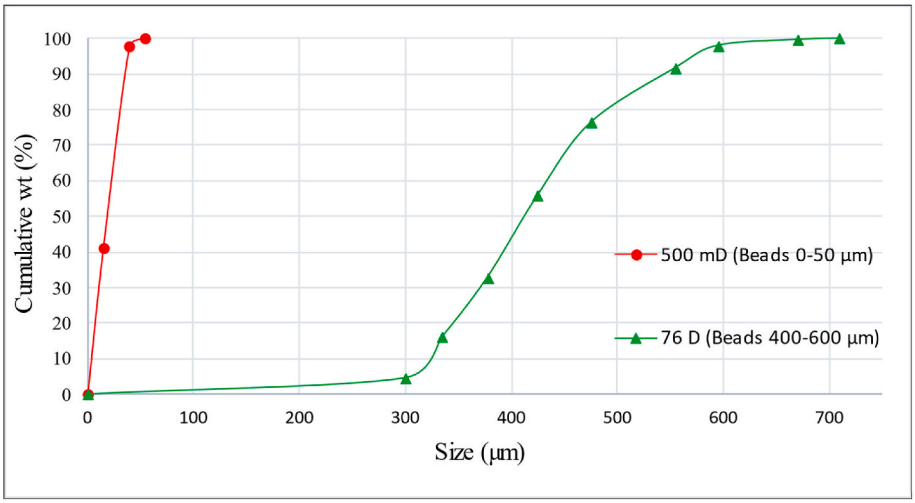

Fig. 5. Particle size distribution of the glass beads.

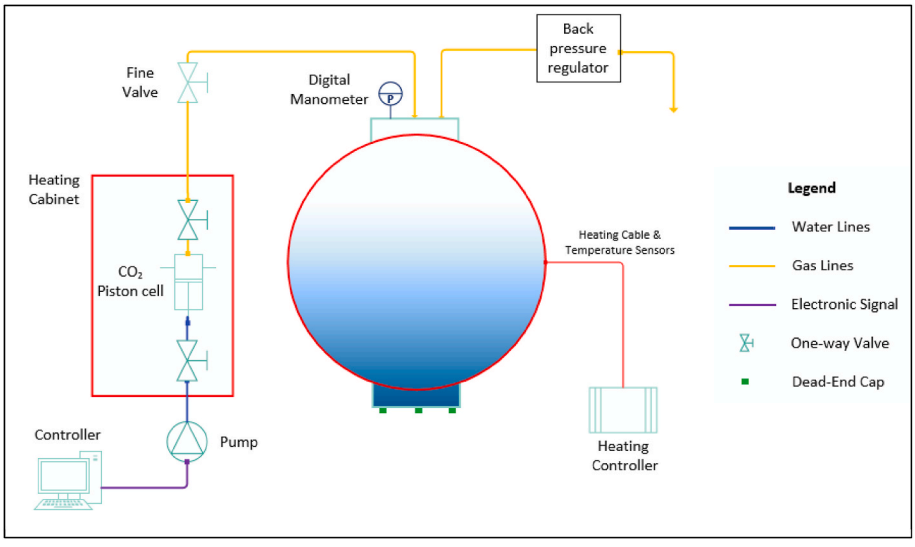

Fig. 6. Piping and instrumentation (P & ID) diagram of the experimental setup.

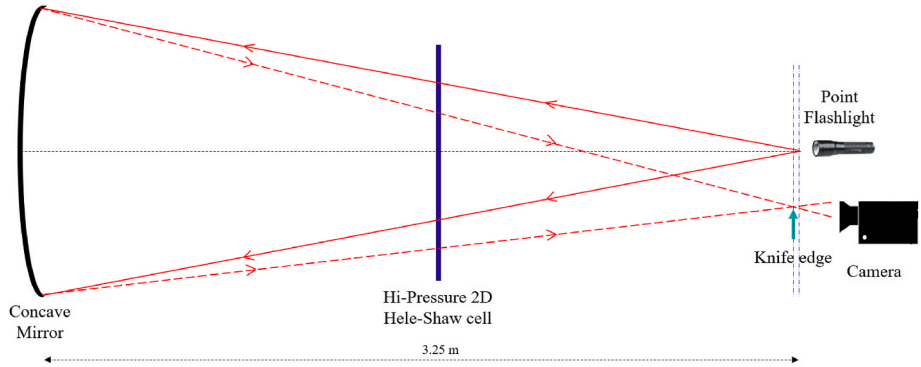

Fig. 7. Schematic sketch of the Schlieren imaging setup.

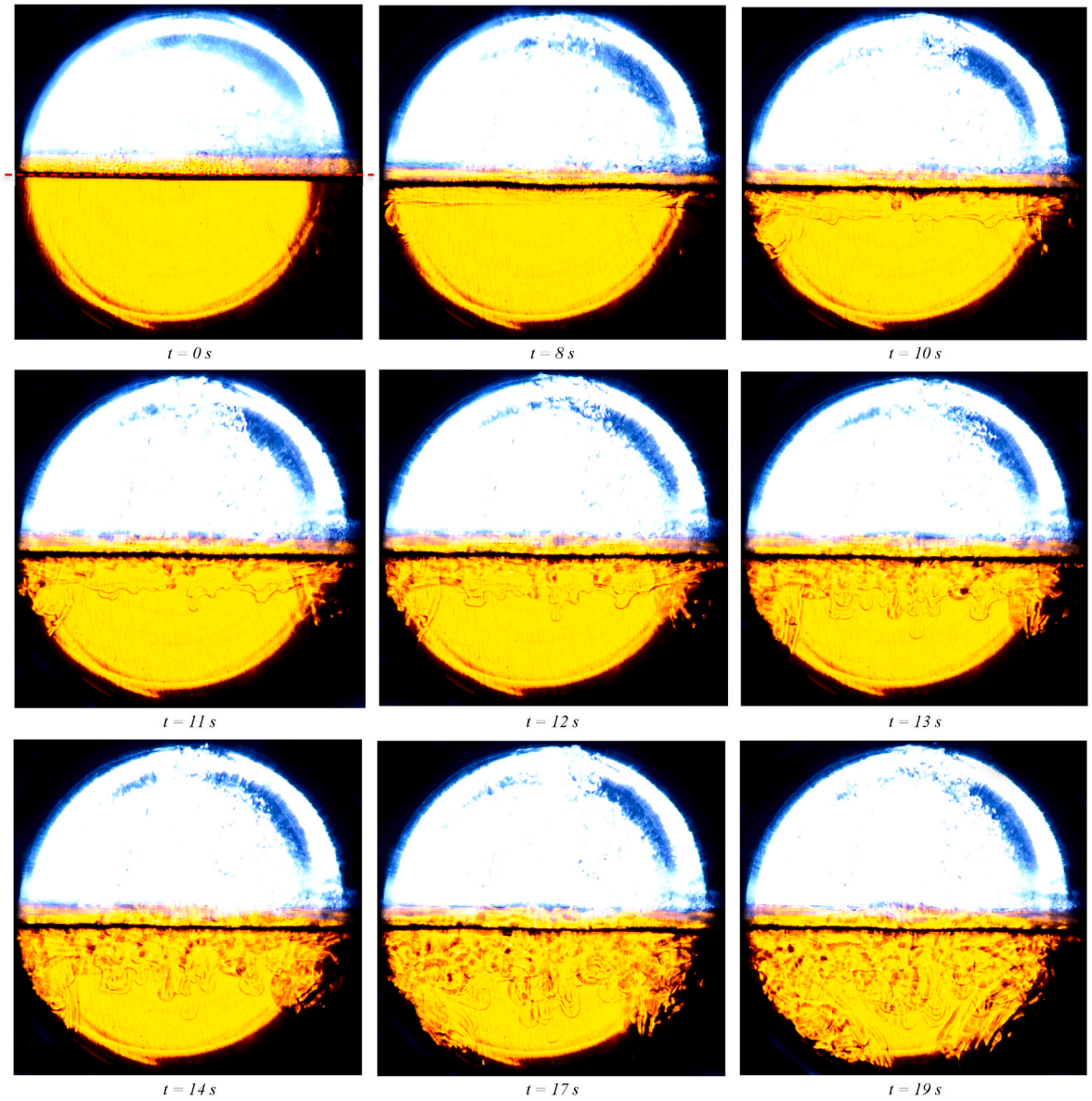

Fig 8. Case 1 – Visual snaps from CO_2/n-decane system without porous media. The red dotted line at t=0 s indicates the initial CO_2/n-decane interface.

Furthermore, this is the CO_2 convective experiments have been carried out with the presence of porous media together with oil which none of the previous studies have been unable to address. A practical outcome of the experimental results will be the visual quantification of CO_2 convective fingers inside oil together with oil swelling. The experiments results will be important in identifying field-scale impacts and

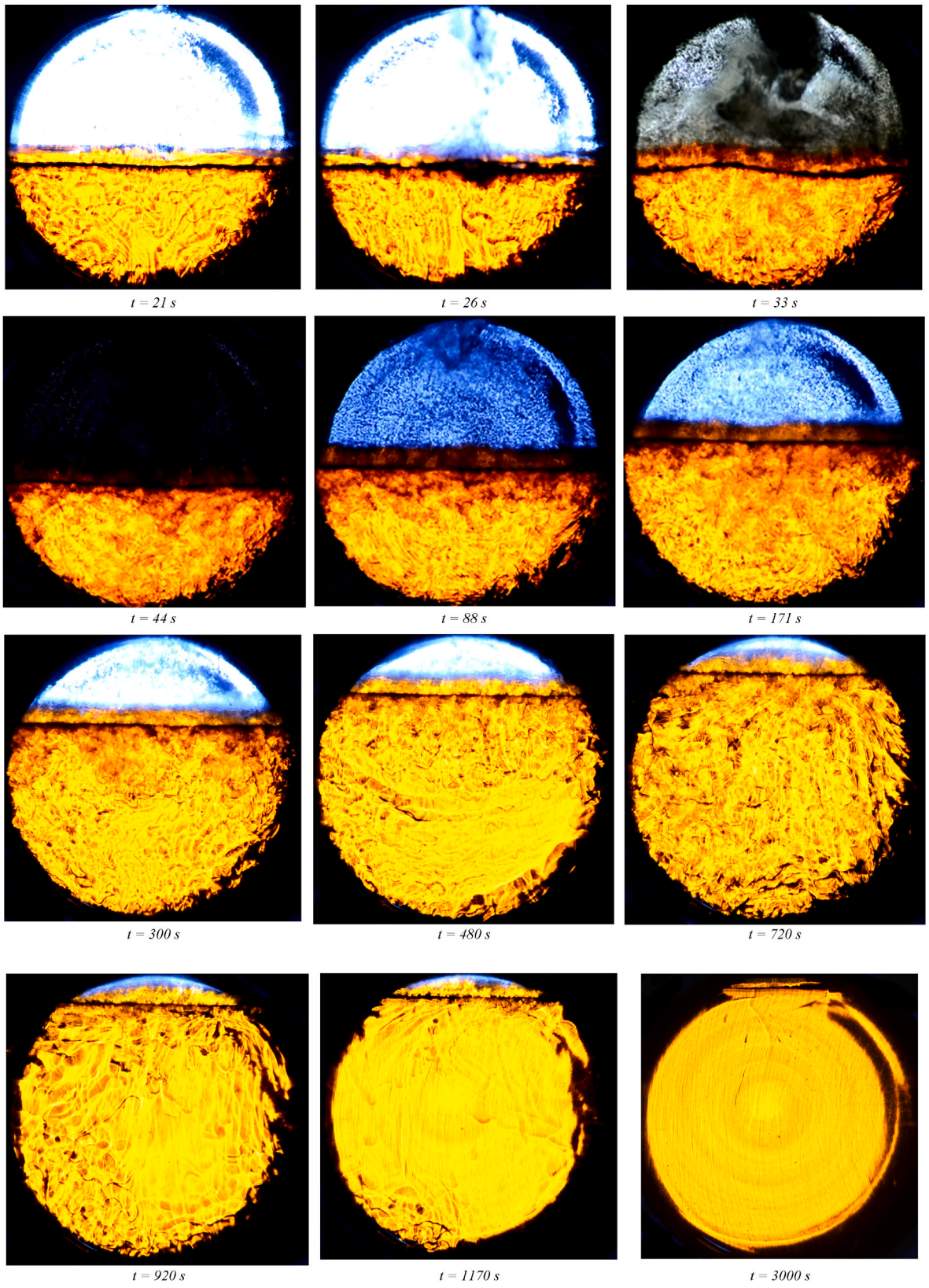

Fig 8. (*continued*).

assessment of reservoir conditions through numerical simulations under which oil and gas recovery can be improved while simultaneously increasing the long-term CO_2 storage potential.

Table 1
Set of experimental cases at 50 °C and 100 bars.

Test #	Fluid(s)	Porous media	Visual results
Case 1	n-decane	–	Figs. 8 and 9
Case 2	n-octane	–	Fig. 10
Case 3	n-decane and water	–	Fig. 13
Case 4	crude oil	–	Fig. 11
Case 5	n-decane	76 D	Fig. 14
Case 6	n-decane	500 mD	Fig. 15
Case 7	crude oil	76 D	Fig. 16

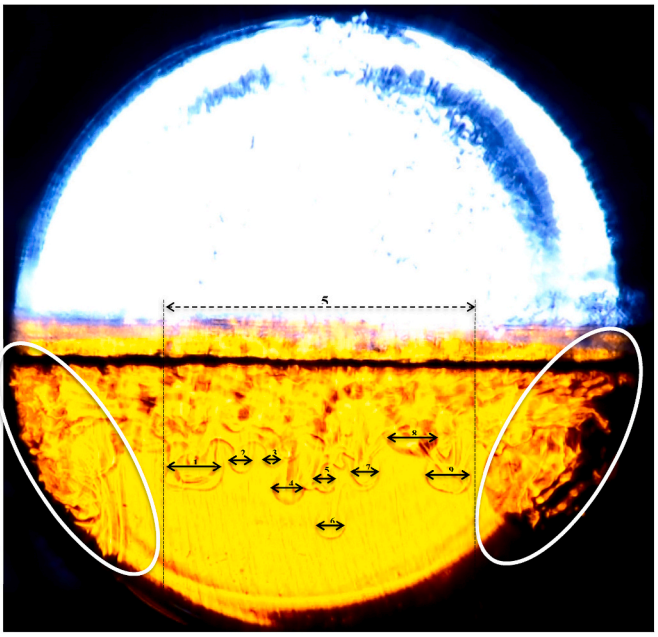

Fig 9. CO_2 convective fingers at t=14 s for n-decane system without porous media (case 1). Distinguishable fingers are marked in arrows and widths are given in Table. 2. White circles indicate how CO_2 mix along the boundary due to boundary effects.

2. Method

2.1. High-pressure 2D cell

The high-pressure 2D-cell was developed using stainless duplex steel and borosilicate glass. The 2D cell was designed for maximum working conditions of 150 bars and 100 °C. The test cell consists of several units, which are assembled to construct the final cell. The cell volume was formed by two glass plates separated by an adjustable spacer. A heating cable was wrapped around the cell with an automatic temperature controller. The front view of the real cell with insulation is shown in Fig. 2. A 3D sketch of the cell is shown in Fig. 4 while a cross-section of the cell is shown in Fig. 3. A specially designed filter module of shaped glass filter (pore size of 10–16 μm) plate was placed at the inlet and outlet to avoid penetrating the glass beads away from the test volume (see Figure 3 and 4). The location of the gas injection was placed in the middle of the top filter module unit as shown in Fig. 3. The diameter of the test volume is 200 mm while the sight disk glass diameter was 100 mm. The thickness is 5.0 mm. Amarasinghe et al. (2020) has provided further details of the high-pressure 2D cell and its design specifications.

2.2. Materials

2.2.1. Chemicals

N-decane, n-octane, and a North Sea crude oil were used as oils. To improve the visualization of the oil phase (with n-decane and n-octane), the oil-soluble dye Sudan III (0.04 wt%) was added to the oils. Aqueous 0.04 wt% bromothymol blue (BTB) pH indicator solution (deionized water mixed with 0.01M NaOH and BTB) of pH around 8 was used as the water phase. The BTB pH indicator is blue above pH = 7.6 and yellow below pH = 6.5, and green between these pH-values (De Meyer et al., 2014). When CO_2 is dissolved in water, the pH will be reduced due to the release of H^+ ions which will lead to the colour change in the water phase from blue to yellow (Thomas et al., 2015). Due to the high light intensity, the colour transition to yellow was visible as dark black colour.

2.2.2. Porous media

Hydrophilic glass beads of different diameters were used to prepare porous media of different permeabilities (500 mD and 76 D). Fig. 5 shows the particle size distribution of each porous media type. The porosity and the permeability of the bead packs was determined by the waterflooding of tubes with packed porous media.

2.3. Experimental procedure

The experimental set-up with the high-pressure 2D test cell is shown in the piping and instrumentation diagram (P & ID) (see Fig. 6). A back-pressure regulator was included in the set-up to avoid sudden developments of high pressures inside the cell. CO_2 was introduced from a piston cell. A digital manometer was connected directly to the 2D cell for accurate reading of the absolute pressure.

All the experiments were carried out at 50 °C and 100 bars. 2D Hele-Shaw cell was pre-heated using the heating cables up to 50 °C. All the fluids were pre-heated inside a heating cabinet (at 50 °C) before adding them into the Hele-Shaw cell. To observe CO_2 convective dissolution in oil, a known volume of oil (n-decane, n-octane, crude oil) was filled into the cell manually. In the CO_2 dissolution experiment with n-decane, a water layer at the bottom was first filled into the cell followed by n-decane.

For the experiments with porous media, the test volume is filled with a known volume of oil first. And then, dry glass beads were filled manually from the top of the cell gradually so that the beads will settle smoothly inside the oil phase (filling dry glass beads first and flood oil through to saturate the pack was not possible due to uneven packing and possible cracking inside the porous media). When the desired level of porous media was achieved, small external vibration was applied to the cell by using a plastic hammer to further settle the glass beads. If any oil was above the porous media, it was sucked out using a syringe. After placing the filter module on the top of the cell, the cell was left for approximately half an hour to get even packing of the homogenous porous media and stable temperature (confirmed from a thermal image by a FLUKE® Ti25 thermal imaging camera).

The CO_2 piston cell was first filled to 80 bars at room temperature and then heated to 50 °C. After the gas expansion, the piston cell was pressurized to 105 bars. The fine valve connected to the CO_2 piston cell (see Fig. 6), was then opened slowly to allow CO_2 to flow into the 2D cell to avoid the splash of CO_2 into the liquid phase and movement of glass beads.

The visualization observations were carried out using the Schlieren method using a Nikon D5200 camera with video recording. ImageJ open-source image analysis software (Rueden et al., 2017) was used to analyze the width of CO_2 convective fingers and oil swelling due to CO_2 mixing. To measure the oil swelling, the height increase of the free oil phase was measured using the software and was converted to the volume.

2.4. Schlieren method

2.4.1. Theory of schlieren method

The Schlieren method has been used by (Thomas et al. 2015, 2018)

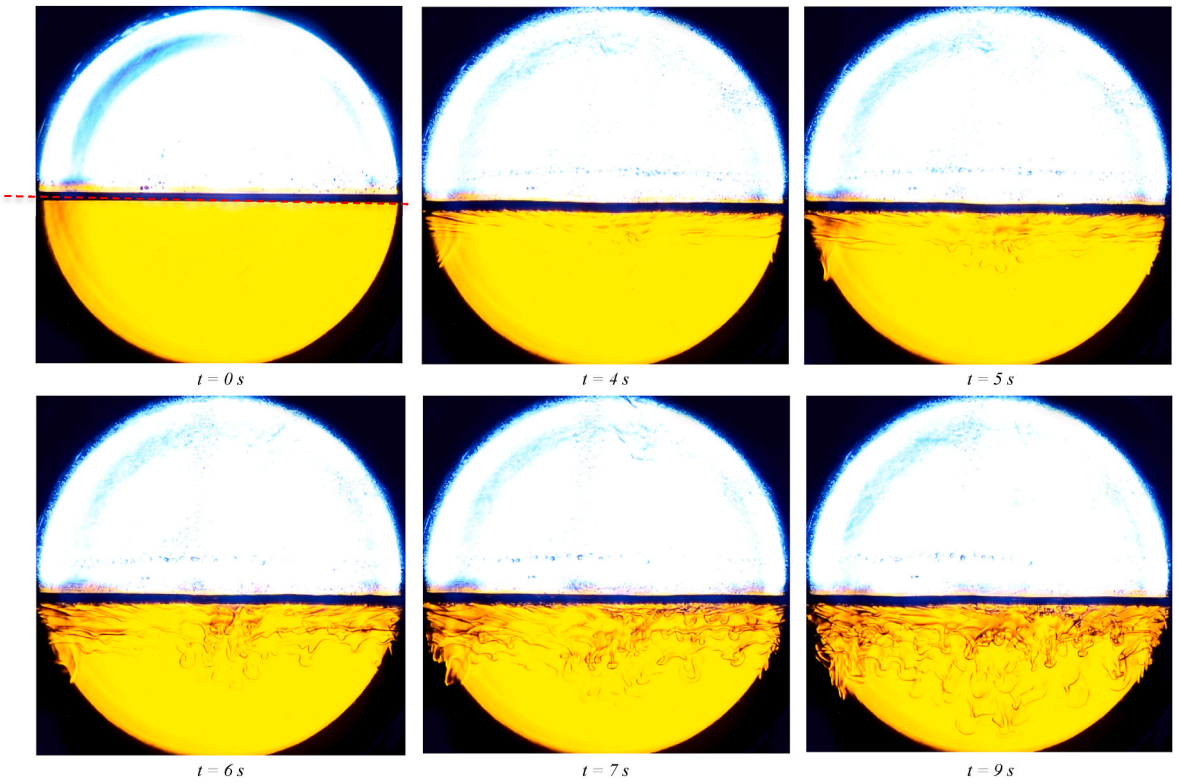

Fig 10. Case 2 - CO2/n-octane system without porous media. The red dotted line at t=0 s indicates the initial CO_2/n-octane interface.

to visualize CO_2 convective dissolution in water and salt solutions inside a Hele-Shaw cell at ambient conditions. Detecting the deflection of the light beam sent via the cell is the basic principle of the Schlieren method. The density gradients occur due to the fluid mixing (CO_2/Oil in this case) is the reason for the deflection of the light beam. One of the drawbacks of the Schlieren method is that it can be only applicable to bulk fluid flows setup. i.e. cannot be applied with the presence of porous media. See Settles (2001) and Bunton et al. (2016) for more general information on the Schlieren method.

To visualize flow inside a 2D Hele-Shaw experimental setup, the Schlieren method can be applied in several ways depending on how the concave mirrors or convex lenses are used.

Method 1: Two convex lenses method (Khosrokhavar et al., 2014; Thomas et al. 2015, 2018)
Method 2: Two concave mirrors method (Eder and Jordan, 2001; Settles, 2001)
Method 3: Single concave mirrors method (Eder and Jordan, 2001; Settles, 2001)

2.4.2. Application of schlieren method for this study

As our visualization window of the 2D Hele-Shaw cell is large (i.e. 10 cm), above mentioned (see subchapter 2.4.1) two Schlieren visualization methods were not possible to use because of the requirement of either two concave mirrors or two convex lenses with a larger diameter. Due to the lack of space in our lab, we (have opted for a Schlieren visualization method that uses only a single concave mirror. According to the requirement, a single concave mirror of diameter 20.32 cm and an effective focal length of 162.56 cm was used.

The mechanism of the Schlieren method using a single concave mirror is described as follows (see Fig. 7). A point light source is applied from the front side of the cell as the main light source. The light source was placed at 2 times the focal length of the concave mirror. Before the start of the experiment, the deflected light beam coming from the concave mirror was converged to the pre-arranged knife-edge where the camera was focused on the converging light source.

During the experiment, light rays are deflected due to the refractive index variation caused by the CO_2/oil mixture. The light rays coming through the experimental 2D cell glass are scrambled due to the CO_2 concentration variation. These oncoming light rays will not exactly be focused on the two times of the focal length of the mirror but on a focal plane to the mirror. So, by adjusting the knife-edge the perfect focal point can be found so that any light rays will not get lost which could lead to loss of the image intensity. Then to obtain the images the camera was used. In Fig. 7, a schematic sketch of the applied Schlieren method for this experiment is shown.

2.5. Set of experiments

Seven sets of CO_2 convective dissolution experiments were carried out as shown in Table 1.

3. Results and discussion

3.1. Visual observations of CO_2 dissolution into the oil without porous media

CO_2 was introduced to the oil phase of n-decane (Fig. 8). Due to the time delay in the opening of the fine valve slowly, CO_2 starts to have the first contact with the oil phase at t = 8 s. Then after, sudden development of CO_2 fingering was observed into the oil phase (see t = 10 s in Fig. 8). The fingers were observed drawn towards the bottom of the cell due to the gravity-driven mechanism until 17 s. In Fig. 9, an enlarged image of CO_2 convective fingers at t = 14 s is shown. The width of the fingers was counted and measured (see Table 2). Within a 5 cm span, 9 fingers were distinguished. The width of the fingers was observed as random. Meanwhile, the fingers were observed to merge with time, and the width of the fingers and locations were continuously changing.

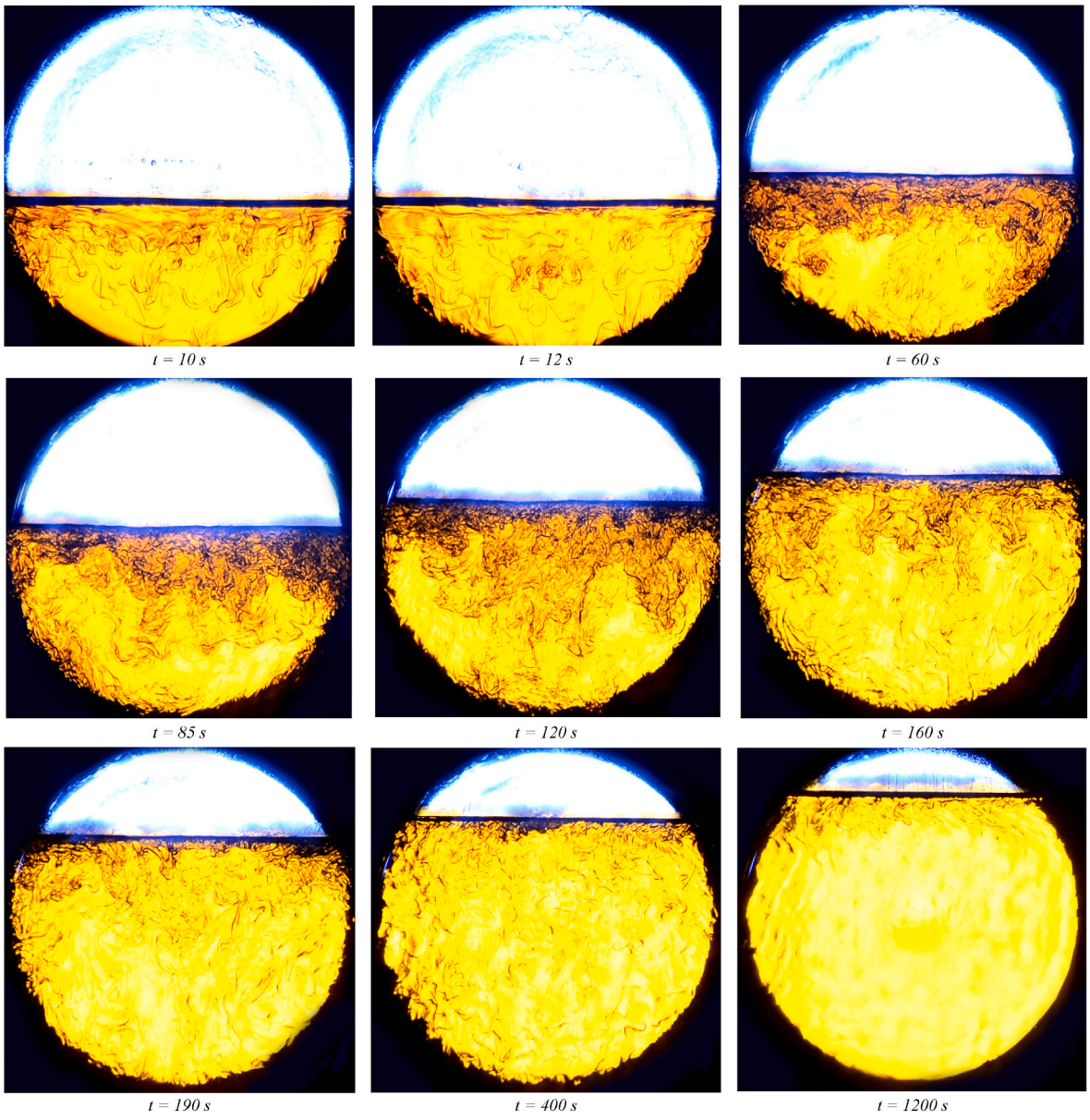

Fig 10. (*continued*).

The circular boundary affects the direction of CO_2 fingers downwards (see CO_2 flow along the boundary in Fig. 9 circled in white colour). At t = 17 s and t = 19 s, CO_2 reaches the bottom of the cell along the boundary before the middle fingers reach the bottom. At t = 21 s the CO_2 came along the left and right side of the boundaries merge with the centre fingers. At t = 26 s, the merged convective flow of CO_2 reaching upwards through the centre of the cell was observed.

From t = 33 s to t = 88 s, a disturbance to the oil phase was observed due to the phase change of CO_2, i.e. from the time of opening the fine valve slowly and up to t = 33 s CO_2 behaves as a gas phase. With time when CO_2 filled up the 2D cell space, CO_2 changes its phase-type from gas to liquid followed by the supercritical phase. From t = 171 s (after the disturbance) CO_2 convective fingers were circulating inside the oil phase. Meantime more CO_2 was dissolved into the oil phase. This can be observed by comparing the oil level at t = 8 s and t = 3000 s. With time the CO_2 convective fingers got less concentrated which indicated that the oil phase was getting fully saturated with CO_2. At t = 1170 s, less amount of CO_2 convective fingers can be observed. At t = 3000 s a fully saturated oleic phase with CO_2 can be observed. Due to the presence of the high-pressure CO_2, the dissolution process was instantaneous. N-decane swelling was calculated at the end of the experiment to be 55%.

The same behaviour as for n-decane was observed for n-octane (see Fig. 10). In Fig. 10 images from disturbance that occurred due to the phase change of CO_2 were omitted which happens between t = 12 s and t = 60 s. It was observed that CO_2 dissolution in n-octane was faster than for n-decane. The whole convective dissolution process was finished in about half time compared to n-decane for the same amount of oil volume. N-octane swelling was calculated at the end of the experiment to be 50%.

CO_2 convective dissolution into crude oil experiment was also conducted (see Fig. 11). Due to the thick dark colour intensity of crude oil, light cannot penetrate the crude oil. So, CO_2 convective dissolution fingers and convection flows cannot be identified using the Schlieren method. The swelling of crude oil was calculated as 11% at the end of the experiment.

3.2. Visual observations of CO_2 dissolution into the oil with a water layer without porous media

Another experiment was carried out with n-decane on top of the

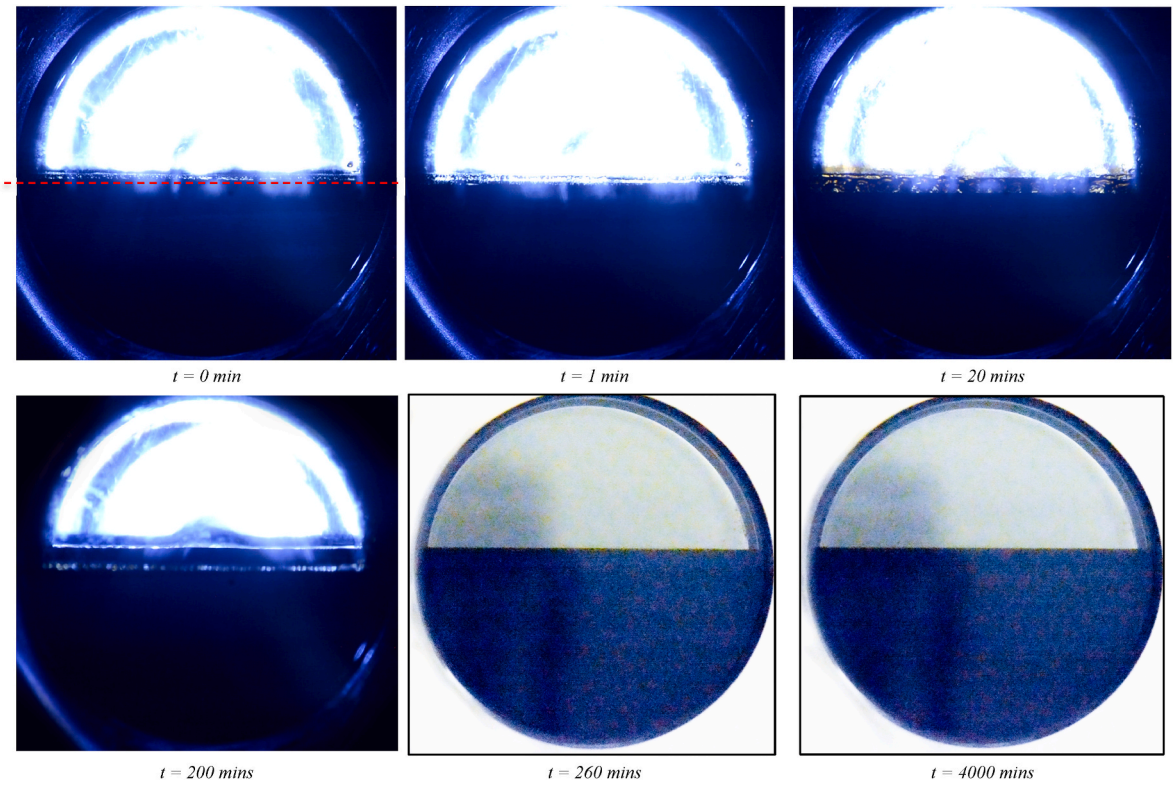

Fig. 11. Case 4 - CO_2/crude oil system without porous media. The red dotted line at t=0 s indicates the initial CO_2/crude oil interface.

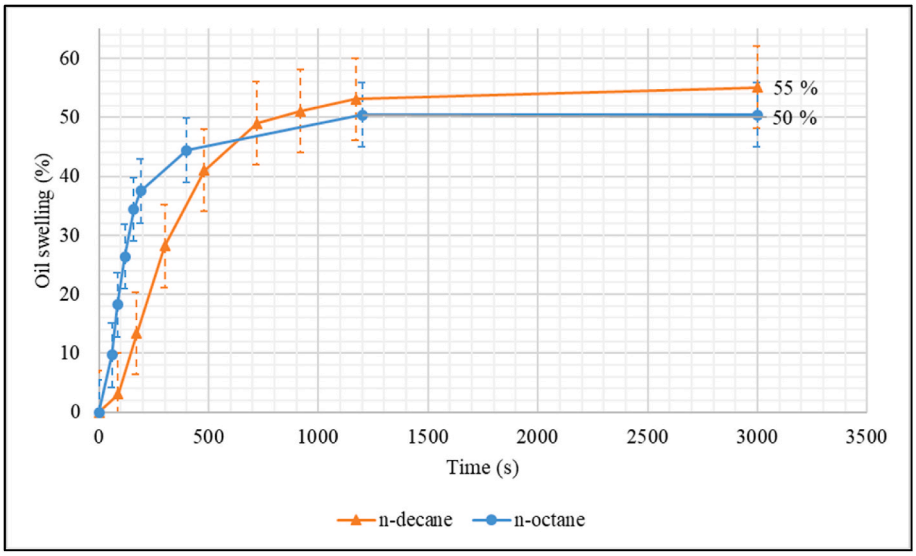

Fig. 12. Oil swelling percentages for n-decane (case 1) and n-octane (case 2) without the presence of porous media. Error bars are given as standard error.

water phase. Experimental images at different stages are given in Fig. 13. First, at the introduction of CO_2, CO_2 fingering was observed in n-decane (as explained earlier). At t = 15 s, CO_2 came along the boundaries level off on the top of the n-decane/water fluid's plane. The merged CO_2 together with incoming CO_2 fingers along the middle of the oil phase started convective fingers upwards. At t = 42 s, CO_2 convective fingers into the water phase were observed (notice the small black fingers right below the water phase at t = 42 s). Several fingers were developed downwards up to t = 59 s while several fingers were merging when they reached the bottom. Boundary effects also were observed when CO_2 was dissolved into the water phase. Similar observations were made by Amarasinghe et al. (2020) when they visualized CO_2 dissolution into the water phase at the same pressure and temperature conditions (50 °C and 100 bar). From t = 49 s to t = 135 s, the water phase became saturated with CO_2 which changed the colour of the water phase from blue to yellow. Meanwhile, CO_2 convective fingers kept flowing in n-decane, and swelling of the oil phase continued. At t = 1200 s almost all the n-decane phase was observed saturated. Since 50 ml of n-decane was used compared to the previous case with 100 ml, the whole CO_2 convective dissolution process was finished faster, approximately in half the time with 100 ml n-decane.(see Fig. 12)

Table 2
CO_2 convective finger's width at t = 14s for the n-decane system without porous media (case 1) as per Fig. 9.

Finger #	The width of the finger (mm)
1	9.25
2	3.80
3	3.20
4	5.30
5	4.20
6	4.85
7	4.56
8	8.26
9	7.32

3.3. Visual observations of CO_2 dissolution into oil with porous media

CO_2 convective dissolution into porous media was observed for 3 different cases. In the first, CO_2 was introduced to 100% n-decane saturated 76 D porous media (55 ml of n-decane was used). In the beginning, the levels of the porous media and n-decane were the same (see t = 0 min in Fig. 14). As mentioned in the introduction, the Schlieren method can only be applied for bulk fluids. Since light does not penetrate through porous media, CO_2 convective fingers inside porous media cannot be obtained using the Schlieren method. During this study, we have attempted to add a CO_2 soluble dye (C.I. Disperse Red 60) in the CO_2 phase in order to track CO_2 transport in oil-saturated porous media. But due to the lower solubility of the dye in CO_2 at 100 bar (our working pressure), the attempt was unsuccessful (Gupta and Shim, 2007).

When CO_2 was dissolved into the n-decane phase with time, the n-decane phase began to swell and produce a free n-decane phase above the porous media. CO_2 convective flows were observed inside the swelled free n-decane (see at t = 5 min in Fig. 14). With further time at t = 10 min and t = 20 min, n-decane kept swelling as well as CO_2 convective flow kept circulating inside the oil phase. At t = 170 min, CO_2 swelling has stopped along with further CO_2 convective flows in the oil phase which indicated all the oil inside porous media, as well as swelled oil, has been fully saturated with CO_2. A total oil swelling of 46% was calculated from the image analysis. Fig. 17 shows the oil swelling percentage as a function of time for the experiment case 5.

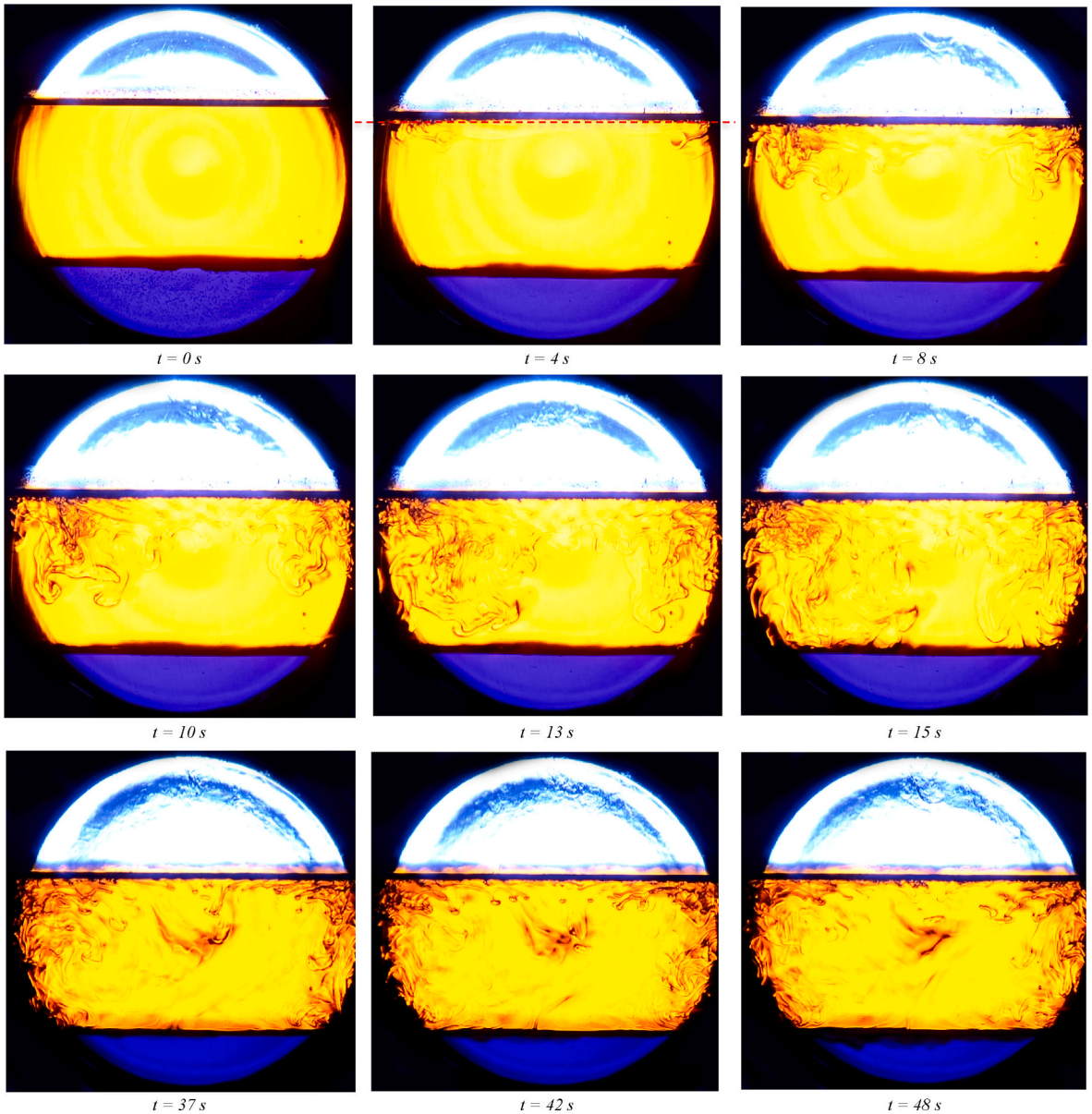

Fig. 13. Case 3 - CO_2/n-decane/Water system without porous media. The red dotted line at t=4 s indicates the initial CO_2/n-decane interface.

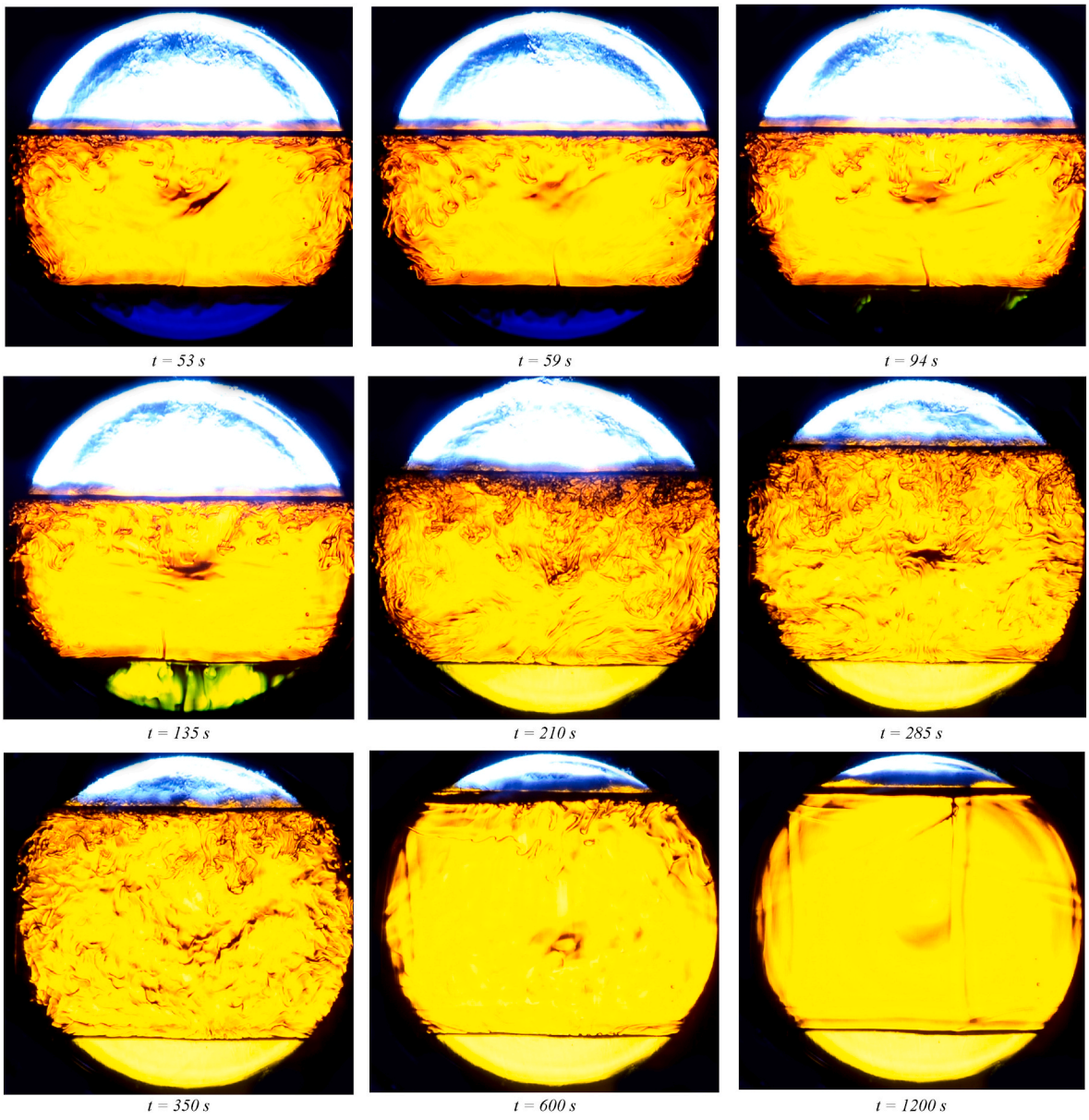

Fig. 13. (*continued*).

A similar experiment was carried out for n-decane (55 ml) saturated porous media of 500 mD (see Fig. 15). Similar observations were observed as in 76 D porous media. In order to fully saturate oil with CO_2 and stop the swelling of oil, it took 2000 min in 500 mD porous media which is approximately 117 times slower than in 76 D porous media. A total oil swelling of 32% was calculated from the image analysis. The difference of oil swelling between 76 D and 500 mD was understood as due to the small differences in the porosity.

CO_2 convective dissolution was studied also for 76 D porous media saturated with crude oil (55 ml) (see Fig. 16). Since it was understood that CO_2 convective flow cannot be seen even in the swelled oil phase, general images of the experiment were taken instead of using the Schlieren method. Only a small fraction of oil swelling was observed even after 2000 min of the experiment.

4. Suggested future work

Visualization of CO_2 convective mixing/fingers inside oil-saturated porous media using a Hele-Shaw cell yet to be achieved experimentally. With the use of high-tech such as X-ray or MRI technology, it may be possible to visualize CO_2 convective fingering inside porous media. Moreover, usage of reservoir rock types is recommended to investigate both CO_2 convective mixing and fluid-rock interactions together. Furthermore, the experimental results will be used to improve the numerical simulation which are developed using the Open Porous Media (OPM) framework (Lauser, 2014; Rasmussen et al., 2020).

5. Conclusions

- The available high-pressure 2D-cell and Schlieren imaging method have made it possible to investigate CO_2-dissolution and convective mixing into oil phases at pressures and temperatures realistic for reservoirs with CO_2-EOR and CO_2-storage.
- Convective fingering was found to contribute to the mixing of CO_2 into n-octane and n-decane without porous media. CO_2 convective fingering was not possible to visualize with crude oil due to the low opacity of the oil phase. The CO_2 dissolution into oil phases was quite fast without porous media.

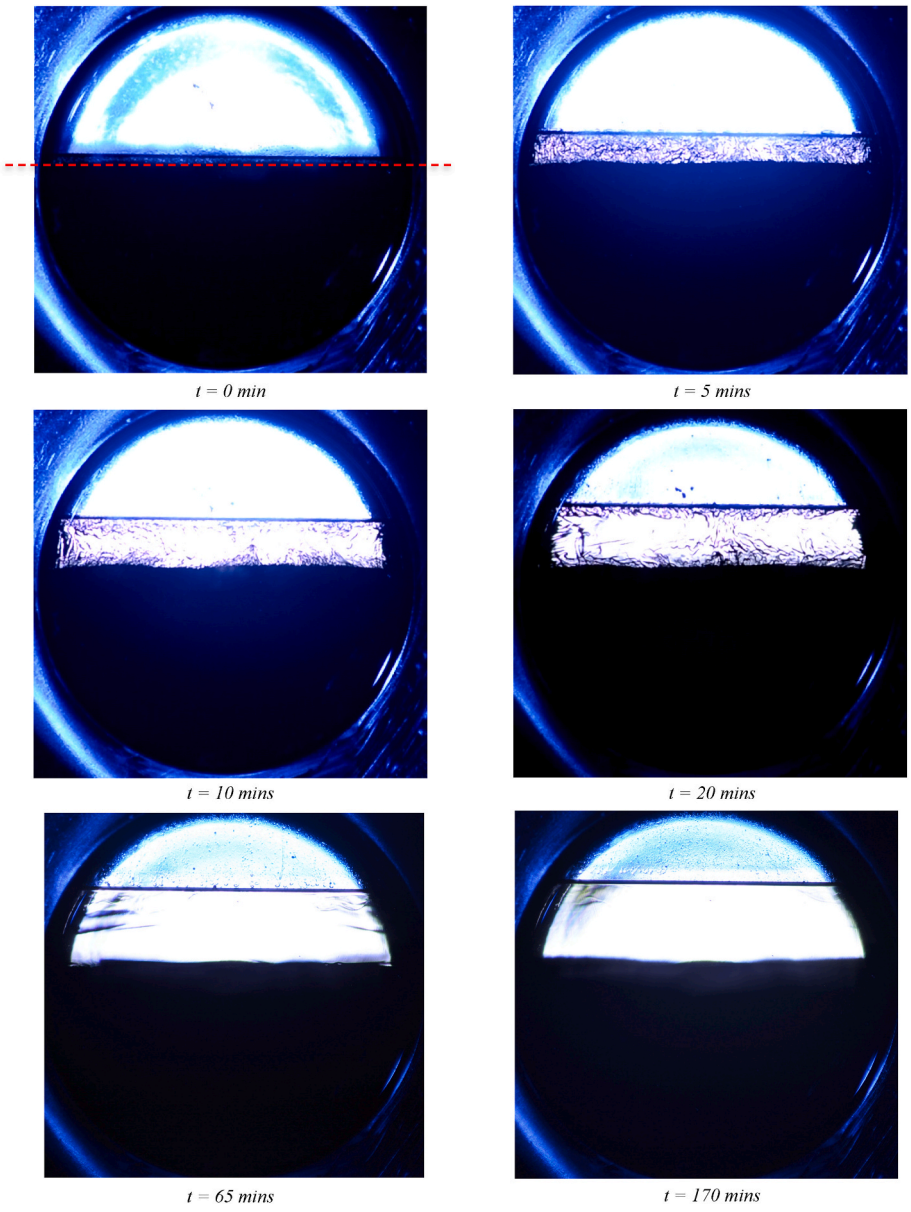

Fig. 14. Case 5 - Experimental snapshots of CO_2/n-decane system with 76 D porous media. The red dotted line at t=0 s indicates the level of porous media.

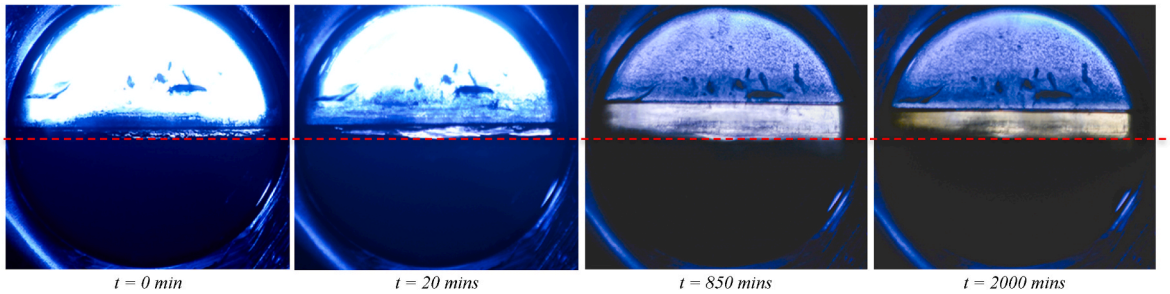

Fig. 15. Case 6 - CO_2/n-decane system with 500 mD porous media. The red dotted line indicates the level of porous media.

- At the end of the CO_2 mixing process, the swelling of the oil phase was 55% for n-decane and 50% for n-octane. Much less oil swelling was observed for crude oil which was calculated as 11%.
- Boundary effects were affecting the CO_2 dissolution process due to the circular shape of the 2D-cell.
- An oil phase above the water phase tends to damp the CO_2 dissolution transition process from the oil phase to the water phase.
- The CO_2 dissolution into oil-saturated porous media was slower compared to without porous media. The mixing of CO_2 was faster at higher permeability than at lower permeability.

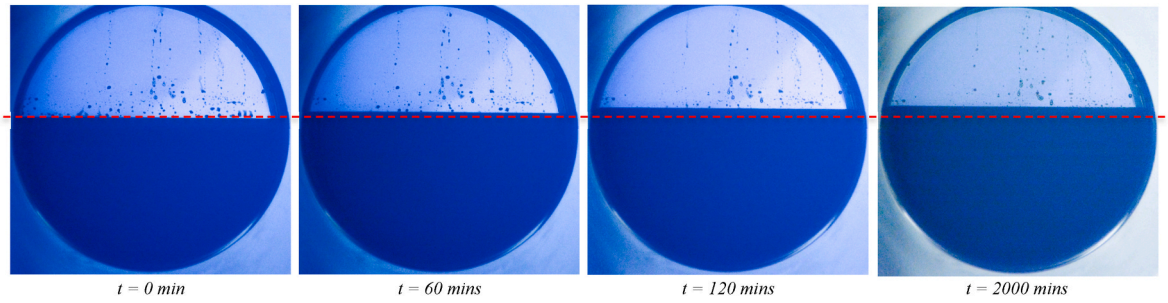

Fig. 16. Case 7 - CO_2/crude oil system with 76 D porous media. The red dotted line indicates the level of porous media.

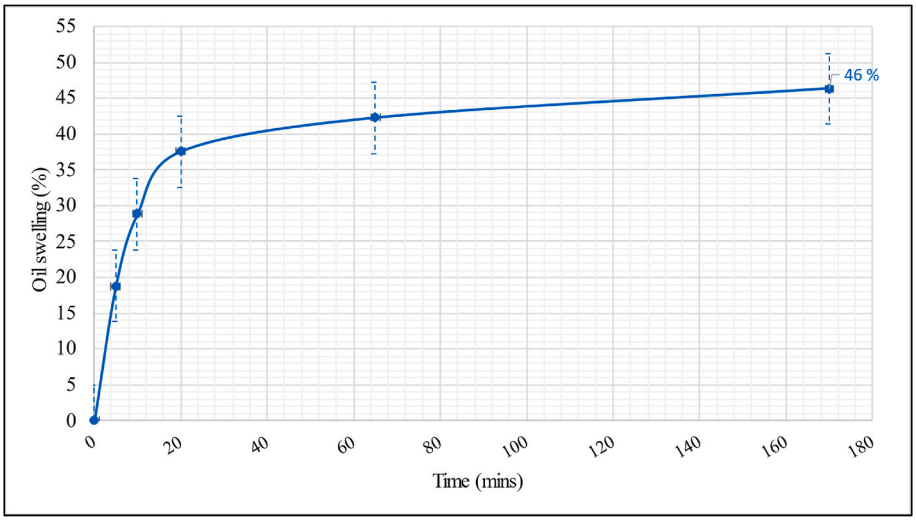

Fig. 17. Swelling of the oil phase for the CO_2/n-decane system for experiment case 5 with 76 D porous media. Error bars are given as standard error.

- Oil swelling of 46% and 32% was observed with n-decane saturate porous media with 76 D and 500 mD respectively. CO_2 mixing process was 117 times slower in 500 mD compared to 76 D to fully saturate oil with CO_2 and stop the swelling of oil.
- The experiment results will further make it possible to better define and validate the simulation model for upscaling procedures for CO_2 storage and EOR.

Author statement

Widuramina Amarasinghe:Conceptualization, Methodology, Validation, Investigation, Writing, Visualization, Formal analysis. Ingebret Fjelde: Conceptualization, Methodology, Validation, Investigation, Writing, Supervision, Funding acquisition. Ying Guo: Conceptualization, Methodology, Writing, Supervision, Project administration, Funding acquisition

Declaration of competing interest

The authors declare that they have no known competing financial interests or personal relationships that could have appeared to influence the work reported in this paper.

Acknowledgment

The authors would like to thank the Research Council of Norway for the funding of this research project through the CLIMIT program which is dedicated to the accelerating and the commercialization of Carbon Capture and Storage (CCS) through research, development, and demonstration.

References

Agartan, E., Trevisan, L., Cihan, A., Birkholzer, J., Zhou, Q., Illangasekare, T.H., 2015. Experimental study on effects of geologic heterogeneity in enhancing dissolution trapping if supercritical CO_2. Water Resour. Res. 51 (3), 1635–1648. https://doi.org/10.1002/2014WR015778.

Amarasinghe, W., Farzaneh, S., Fjelde, I., Sohrabi, M., Guo, Y., 2021a. A visual investigation of CO_2 convective mixing in water and oil at the pore scale using a micromodel apparatus at reservoir conditions. Gas 1 (1), 53–67. https://doi.org/10.3390/gases1010005.

Amarasinghe, W., Fjelde, I., Giske, N., Guo, Y., 2021b. CO_2 convective dissolution in oil-saturated unconsolidated porous media at reservoir conditions. Energies 14 (1), 233. https://doi.org/10.3390/en14010233.

Amarasinghe, W., Fjelde, I., Rydland, J.-Å., Guo, Y., 2020. Effects of permeability on CO_2 dissolution and convection at reservoir temperature and pressure conditions: a visualization study. Int. J. Greenh. Gas. Control 99, 103082. https://doi.org/10.1016/j.ijggc.2020.103082.

Bachu, S., 2008. CO_2 storage in geological media: role, means, status and barriers to deployment. Prog. Energy Combust. Sci. 34 (2), 254–273. https://doi.org/10.1016/j.pecs.2007.10.001.

Blunt, M., Fayers, F.J., Orr, F.M., 1993. Carbon dioxide in enhanced oil recovery. Energy Convers. Manag. 34 (9), 1197–1204. https://doi.org/10.1016/0196-8904(93)90069-M.

Brock, W.R., Bryan, L.A., 1989. Summary Results of CO_2 EOR Field Tests, 1972-1987. Paper presented at the Low Permeability Reservoirs Symposium, Denver, Colorado. https://doi.org/10.2118/18977-MS.

Budinis, S., Krevor, S., Dowell, N.M., Brandon, N., Hawkes, A., 2018. An assessment of CCS costs, barriers and potential. Energy Strategy Rev. 22, 61–81. https://doi.org/10.1016/j.esr.2018.08.003.

Bunton, P., Marin, D., Stewart, S., Meiburg, E., De Wit, A., 2016. Schlieren imaging of viscous fingering in a horizontal hele-shaw cell. Exp. Fluid 57 (2), 28. https://doi.org/10.1007/s00348-016-2121-0.

Cheng, P., Bestehorn, M., Firoozabadi, A., 2012. Effect of permeability anisotropy on buoyancy-driven flow for CO_2 sequestration in saline aquifers. Water Resour. Res. 48 (9) https://doi.org/10.1029/2012wr011939.

Czarnota, R., Janiga, D., Stopa, J., Wojnarowski, P., 2018. Acoustic investigation of CO_2 mass transfer into oil phase for vapor extraction process under reservoir conditions. Int. J. Heat Mass Tran. 127, 430–437. https://doi.org/10.1016/j.ijheatmasstransfer.2018.06.098.

De Meyer, T., Hemelsoet, K., Van Speybroeck, V., De Clerck, K., 2014. Substituent effects on absorption spectra of pH indicators: an experimental and computational study of sulfonphthaleine dyes. Dyes Pigments 102, 241–250. https://doi.org/10.1016/j.dyepig.2013.10.048.

Doranehgard, M.H., Dehghanpour, H., 2020. Quantification of convective and diffusive transport during CO_2 dissolution in oil: a numerical and analytical study. Phys. Fluids 32 (8), 085110. https://doi.org/10.1063/5.0021752.

Eder, A., Jordan, M., 2001. The schlieren technique. In: Mayinger, F., Feldmann, O. (Eds.), Optical Measurements: Techniques and Applications. Springer Berlin Heidelberg, Berlin, Heidelberg, pp. 5–16. https://doi.org/10.1007/978-3-642-56443-7_2.

Elenius, M.T., Gasda, S.E., 2021. Convective mixing driven by non-monotonic density. Transport in Porous Media. https://doi.org/10.1007/s11242-021-01593-3.

Elenius, M.T., Nordbotten, J.M., Kalisch, H., 2014. Convective mixing influenced by the capillary transition zone. Comput. Geosci. 18 (3), 417–431. https://doi.org/10.1007/s10596-014-9415-1.

Emami-Meybodi, H., Hassanzadeh, H., Green, C.P., Ennis-King, J., 2015. Convective dissolution of CO_2 in saline aquifers: progress in modeling and experiments. Int. J. Greenh. Gas. Control 40 (Suppl. C), 238–266. https://doi.org/10.1016/j.ijggc.2015.04.003.

European Commission, 2019. EU Climate Action. Retrieved from. https://ec.europa.eu/clima/policies/eu-climate-action_en.

Faisal, T.F., Chevalier, S., Bernabe, Y., Juanes, R., Sassi, M., 2015. Quantitative and qualitative study of density driven CO_2 mass transfer in a vertical hele-shaw cell. Int. J. Heat Mass Tran. 81 (Suppl. C), 901–914. https://doi.org/10.1016/j.ijheatmasstransfer.2014.11.017.

Farajzadeh, R., Salimi, H., Zitha, P.L.J., Bruining, H., 2007. Numerical simulation of density-driven natural convection in porous media with application for CO_2 injection projects. Int. J. Heat Mass Tran. 50 (25), 5054–5064. https://doi.org/10.1016/j.ijheatmasstransfer.2007.08.019.

Fjelde, I., Asen, S.M., 2010. Wettability alteration during water flooding and Carbon dioxide flooding of reservoir chalk rocks. In: Paper Presented at the SPE Europec Featured at 72nd EAGE Conference and Exhibition. https://doi.org/10.2118/130992-MS. Barcelona, Spain.

Gale, J., Kaya, Y., 2003. Greenhouse Gas Control Technologies - 6th International Conference. Elsevier Science. https://books.google.no/books?id=bC3uRNj4A04C.

Gasda, S., Elenius, M.T., 2018. CO_2 convection in oil driven by non-monotonic mixture density. In: Paper Presented at the ECMOR XVI - 16th European Conference on the Mathematics of Oil Recovery. https://doi.org/10.3997/2214-4609.201802239. Barcelona, Spain.

Gibbins, J., Chalmers, H., 2008. Carbon capture and storage. Energy Pol. 36 (12), 4317–4322. https://doi.org/10.1016/j.enpol.2008.09.058.

Gupta, R.B., Shim, J.-J., 2007. Solubility in Supercritical Carbon Dioxide.

Hartline, B.K., Lister, C.R.B., 1977. Thermal convection in a hele-shaw cell. J. Fluid Mech. 79 (2), 379–389. https://doi.org/10.1017/S0022112077000202.

Hassanzadeh, H., Pooladi-Darvish, M., Keith, D.W., 2009. Accelerating CO_2 dissolution in saline aquifers for geological storage — mechanistic and sensitivity studies. Energy Fuel. 23 (6), 3328–3336. https://doi.org/10.1021/ef900125m.

Janiga, D., Czarnota, R., Kuk, E., Stopa, J., Wojnarowski, P., 2020. Measurement of oil-CO_2 diffusion coefficient using pulse-echo method for pressure-volume decay approach under reservoir conditions. J. Petrol. Sci. Eng. 185, 106636. https://doi.org/10.1016/j.petrol.2019.106636.

Khosrokhavar, R., Elsinga, G., Farajzadeh, R., Bruining, H., 2014. Visualization and investigation of natural convection flow of CO_2 in aqueous and oleic systems. J. Petrol. Sci. Eng. 122 (Suppl. C), 230–239. https://doi.org/10.1016/j.petrol.2014.07.016.

Kneafsey, T.J., Pruess, K., 2011. Laboratory experiments and numerical simulation studies of convectively enhanced Carbon dioxide dissolution. Energy Procedia. 4 (Suppl. C), 5114–5121. https://doi.org/10.1016/j.egypro.2011.02.487.

Lauser, A., 2014. Theory and Numerical Applications of Compositional Multi-phase Flow in Porous Media. University of Stuttgart, Germany. https://doi.org/10.18419/opus-516, 228.

Lindeberg, E., Wessel-Berg, D., 1997. Vertical convection in an aquifer column under a gas cap of CO_2. Energy Convers. Manag. 38, S229–S234. https://doi.org/10.1016/S0196-8904(96)00274-9.

Liu, Y., Teng, Y., Lu, G., Jiang, L., Zhao, J., Zhang, Y., Song, Y., 2016. Experimental study on CO_2 diffusion in bulk n-decane and n-decane saturated porous media using micro-CT. Fluid Phase Equil. 417, 212–219. https://doi.org/10.1016/j.fluid.2016.02.034.

Lu, G., Liu, Y., Jiang, L., Ying, T., Song, Y., Wu, B., 2017. Study of density driven convection in a hele-shaw cell with application to the Carbon sequestration in aquifers. Energy Procedia. 114 (Suppl. C), 4303–4312. https://doi.org/10.1016/j.egypro.2017.03.1576.

Lv, P., Liu, Y., Jiang, L., Song, Y., Wu, B., Zhao, J., Zhang, Y., 2016. Experimental determination of wettability and heterogeneity effect on CO_2 distribution in porous media. Greenh. Gas.: Sci. Technol. 6 (3), 401–415. https://doi.org/10.1002/ghg.1572.

Mahmoodpour, S., Rostami, B., Soltanian, M.R., Amooie, M.A., 2019. Effect of brine composition on the onset of convection during CO_2 dissolution in brine. Comput. Geosci. 124, 1–13. https://doi.org/10.1016/j.cageo.2018.12.002.

Mahzari, P., Jones, A.P., Oelkers, E.H., 2019. An integrated evaluation of enhanced oil recovery and geochemical processes for carbonated water injection in carbonate rocks. J. Petrol. Sci. Eng. 181, 106188. https://doi.org/10.1016/j.petrol.2019.106188.

Mahzari, P., Tsolis, P., Sohrabi, M., Enezi, S., Yousef, A.A., Eidan, A.A., 2018. Carbonated water injection under reservoir conditions; in-situ wag-type eor. Fuel 217, 285–296. https://doi.org/10.1016/j.fuel.2017.12.096.

Mintzer, I., 1987. A Matter of Degrees. The Potential for Limiting the Greenhouse Effect. World Resources Institute, Washington, DC. United States. https://www.osti.gov/servlets/purl/6581662.

Mojtaba, S., Behzad, R., Rasoul, N.M., Mohammad, R., 2014. Experimental study of density-driven convection effects on CO_2 dissolution rate in formation water for geological storage. J. Nat. Gas Sci. Eng. 21 (Suppl. C), 600–607. https://doi.org/10.1016/j.jngse.2014.09.020.

Neufeld, J.A., Hesse, M.A., Riaz, A., Hallworth, M.A., Tchelepi, H.A., Huppert, H.E., 2010. Convective dissolution of Carbon dioxide in saline aquifers. Geophys. Res. Lett. 37 (22) https://doi.org/10.1029/2010GL044728.

Pau, G.S.H., Bell, J.B., Pruess, K., Almgren, A.S., Lijewski, M.J., Zhang, K., 2010. High-resolution simulation and characterization of density-driven flow in CO_2 storage in saline aquifers. Adv. Water Resour. 33 (4), 443–455. https://doi.org/10.1016/j.advwatres.2010.01.009.

Rasmussen, A.F., Sandve, T.H., Bao, K., Lauser, A., Hove, J., Skaflestad, B., Klöfkorn, R., Blatt, M., Rustad, A.B., Sævareid, O., Lie, K.-A., Thune, A., 2020. The Open Porous Media flow reservoir simulator. Comput. Math. Appl. https://doi.org/10.1016/j.camwa.2020.05.014.

Rezk, M.G., Foroozesh, J., 2018. Determination of mass transfer parameters and swelling factor of CO_2-oil systems at high pressures. Int. J. Heat Mass Tran. 126, 380–390. https://doi.org/10.1016/j.ijheatmasstransfer.2018.05.043.

Rueden, C.T., Schindelin, J., Hiner, M.C., DeZonia, B.E., Walter, A.E., Arena, E.T., Eliceiri, K.W., 2017. ImageJ2: ImageJ for the next generation of scientific image data. BMC Bioinf. 18 (1), 529. https://doi.org/10.1186/s12859-017-1934-z.

Settles, G.S., 2001. Schlieren and Shadowgraph Techniques. Springer, USA. https://doi.org/10.1007/978-3-642-56640-0.

Seyyedsar, S.M., Sohrabi, M., 2017. Visualization observation of formation of a new oil phase during immiscible dense CO_2 injection in porous media. J. Mol. Liq. 241, 199–210. https://doi.org/10.1016/j.molliq.2017.05.146.

Sohrabi, M., Riazi, M., Jamiolahmady, M., Ireland, S., Brown, C., 2009. Enhanced oil recovery and CO_2 storage by carbonated water injection. In: Paper Presented at the International Petroleum Technology Conference, Doha, Qatar. https://doi.org/10.2523/IPTC-14070-ABSTRACT.

Song, Y., Nishio, M., Chen, B., Someya, S., Ohsumi, T., 2003. Measurement on CO_2 solution density by optical technology. J. Visual 6 (1), 41–51. https://doi.org/10.1007/bf03180963.

Sun, Q., Ampomah, W., Kutsienyo, E.J., Appold, M., Adu-Gyamfi, B., Dai, Z., Soltanian, M.R., 2020. Assessment of CO_2 trapping mechanisms in partially depleted oil-bearing sands. Fuel 278, 118356. https://doi.org/10.1016/j.fuel.2020.118356.

Taheri, A., Torsæter, O., Lindeberg, E., Hadia, N.J., Wessel-Berg, D., 2018. Qualitative and quantitative experimental study of convective mixing process during storage of CO_2 in heterogeneous saline aquifers. Int. J. Greenh. Gas. Control 71, 212–226. https://doi.org/10.1016/j.ijggc.2018.02.003.

Taheri, A., Torsaeter, O., Wessel-Berg, D., Soroush, M., 2012. Experimental and simulation studies of density-driven-convection mixing in a hele-shaw geometry with application for CO_2 sequestration in brine aquifers. In: Paper Presented at the SPE Europec/EAGE Annual Conference. https://doi.org/10.2118/154908-MS. Copenhagen, Denmark.

Teng, Y., Jiang, L., Fan, Y., Liu, Y., Wang, D., Abudula, A., Song, Y., 2017. Quantifying the dynamic density driven convection in high permeability packed beds. Magn. Reson. Imag. 39, 168–174. https://doi.org/10.1016/j.mri.2017.03.004.

Teng, Y., Wang, P., Liu, Y., Jiang, L., Wang, D., 2018. A spectrophotometric method for measuring dissolved CO_2 in saline water. Exp. Fluid 59 (9), 138. https://doi.org/10.1007/s00348-018-2594-0.

Thomas, C., Dehaeck, S., De Wit, A., 2018. Convective dissolution of CO_2 in water and salt solutions. Int. J. Greenh. Gas. Control 72, 105–116. https://doi.org/10.1016/j.ijggc.2018.01.019.

Thomas, C., Lemaigre, L., Zalts, A., D'Onofrio, A., De Wit, A., 2015. Experimental study of CO_2 convective dissolution: the effect of color indicators. Int. J. Greenh. Gas. Control 42 (Suppl. C), 525–533. https://doi.org/10.1016/j.ijggc.2015.09.002.

Tsai, P.A., Riesing, K., Stone, H.A., 2013. Density-driven convection enhanced by an inclined boundary: implications for geological CO_2 storage. Phys. Rev. E - Stat. Nonlinear Soft Matter Phys. 87 (1), 011003 https://doi.org/10.1103/PhysRevE.87.011003.

United Nations, 2015. The Paris Agreement. Retrieved from. https://unfccc.int/sites/default/files/english_paris_agreement.pdf.

Vosper, H., Kirk, K., Rochelle, C., Noy, D., Chadwick, A., 2014. Does numerical modelling of the onset of dissolution-convection reliably reproduce this key stabilization process in CO_2 storage? Energy Procedia. 63, 5341–5348. https://doi.org/10.1016/j.egypro.2014.11.566.

Wang, L., Hyodo, A., Sakai, S., Suekane, T., 2016. Three-dimensional visualization of natural convection in porous media. Energy Procedia. 86 (Suppl. C), 460–468. https://doi.org/10.1016/j.egypro.2016.01.047.

Wei, B., Gao, H., Pu, W., Zhao, F., Li, Y., Jin, F., Sun, L., Li, K., 2017. Interactions and phase behaviors between oleic phase and CO_2 from swelling to miscibility in CO_2-based enhanced oil recovery (EOR) process: a comprehensive visualization study. J. Mol. Liq. 232, 277–284. https://doi.org/10.1016/j.molliq.2017.02.090.

Yassin, M.R., Habibi, A., Zolfaghari, A., Eghbali, S., Dehghanpour, H., 2018. An experimental study of nonequilibrium Carbon dioxide/oil interactions. SPE J. 23 (5), 1768–1783. https://doi.org/10.2118/187093-PA.

Zhang, D., Song, J., 2014. Mechanisms for geological Carbon sequestration. Procedia IUTAM 10, 319–327. https://doi.org/10.1016/j.piutam.2014.01.027.

Zhang, L., Li, X., Ren, B., Cui, G., Zhang, Y., Ren, S., Chen, G., Zhang, H., 2016. CO_2 storage potential and trapping mechanisms in the H-59 block of jilin oilfield China. Int. J. Greenh. Gas. Control 49, 267–280. https://doi.org/10.1016/j.ijggc.2016.03.013.

Zhao, Y., Song, Y., Liu, Y., Liang, H., Dou, B., 2011. Visualization and measurement of CO_2 flooding in porous media using MRI. Ind. Eng. Chem. Res. 50 (8), 4707–4715. https://doi.org/10.1021/ie1013019.